Propagation of quasisolitons in a fiber Bragg grating written in a slow saturable fiber amplifier

Yuval P. Shapira* and Moshe Horowitz
Department of Electrical Engineering, Technion–Israel Institute of Technology, Haifa 32000, Israel
(Received 12 January 2011; published 3 May 2011; corrected 2 June 2011)

We show, by using numerical simulations, that quasisolitons can propagate over a long distance in a fiber Bragg grating that is written in a slow saturable fiber amplifier, such as an erbium-doped fiber amplifier. During the pulse propagation, the front end of the pulse experiences a net gain while the rear end of pulse is attenuated due to the combination of gain saturation and loss. However, the pulse profile almost does not change after propagating over a length of 5 m that is approximately 2500 times larger than the spatial pulse width. The pulse amplitude has an approximately hyperbolic secant profile. We develop a reduced model by using a multiscale analysis to study solitary-wave propagation whennonlinearity and gain are small. When gain saturation also becomes small we find analytically a new family of solitary-wave hyperbolic-secant solutions that approximately solve the reduced model. The solitary waves propagate slightly faster than Bragg solitons that propagate in fiber Bragg gratings without gain and loss.

DOI: 10.1103/PhysRevA.83.053803 PACS number(s): 42.81.Dp

I. INTRODUCTION

Bragg solitons (BSs) are solitary waves that propagate in a uniform fiber Bragg grating (FBG). Such solitons were predicted theoretically [1–4] and then observed in experiments [5,6]. Due to high dispersion that can be obtained in FBGs [5], the peak power of BSs can be high, on the order of tens of kilowatts. Such pulses are advantageous for nonlinear applications such as optical frequency conversion. BSs in the low-intensity limit can be analyzed by using the nonlinear Schrödinger equation that is obtained from the nonlinear coupled mode equations (NLCMEs) by using a multiscale analysis [7,8].

Loss in gratings is caused due to absorption, coupling to cladding modes, and grating imperfections [9]. The loss limits the generation and the minimum propagation velocity of BSs. Erbium-doped fiber amplifiers (EDFAs) are attractive for amplifying signals in the 1.55-μm regime. Therefore, FBGs that are written in EDFAs (BG-EDFAs) can be used to generate and to amplify BSs. In a previous work we have developed a model to study pulse propagation in FBGs written in slow saturable amplifiers, such as erbium-doped fiber amplifiers [10]. We have included in the model the effect of gain saturation on the propagation of a single pulse. We have shown that the saturation effect may not be neglected for BSs. The gain saturation tends to split the input BS into multiple pulses.

Solitary-wave propagation in Bragg gratings with a fast saturable absorber was studied in Ref. [11]. However, in that work the saturation depends on the pulse instantaneous power rather than on the pulse energy, as obtained in BG-EDFAs.

In this paper we show by using numerical simulations that in the presence of loss, slow gain saturation and FBG quasisolitons can propagate in a BG-EDFA. The quasisolitons almost do not change their parameters while propagating over a very long distance. For example, we show that the spatial width, the peak power, and the propagation velocity of the pulse change by up to 0.6% after propagating a length of 5 m in a BG-EDFA that is approximately 2500 times larger than the spatial pulse width.

*yuvalsh@tx.technion.ac.il

In order to understand the propagation of quasisolitons in BG-EDFAs we developed a reduced model by using a multiscale analysis. We found that the propagation of low-intensity pulses in BG-EDFAs can be approximately analyzed by using a modified nonlinear Schrödinger equation that includes saturable-gain and loss terms. When gain saturation also becomes small, we find a family of solitary-wave approximate solutions with a hyperbolic-secant profile. The analytical solutions are in a good quantitative agreement with the results of the full numerical simulations.

The rest of this paper is structured as follows: In Sec. II we describe the results of numerical simulations that demonstrate the propagation of quasisolitons in BG-EDFAs. In Sec. III we use a multiscale analysis and show that in the low-intensity limit, pulse propagation in BG-EDFAs can be approximately described by a modified nonlinear Schrödinger equation that includes saturable gain and loss. We show that when the gain saturation becomes small, a family of solitary-wave functions exists with a hyperbolic-secant profile. In Sec. IV we present the main conclusions.

II. MODEL AND RESULTS OF NUMERICAL SIMULATIONS

Nonlinear pulse propagation along FBGs written in slow saturable amplifiers such as Erbium-doped fiber amplifiers (BG-EDFAs) was studied in Ref. [10]. Assuming that the refractive index change caused by the gain saturation can be neglected, the propagation of pulses in uniform BG-EDFAs can be analyzed by using modified NLCMEs with saturable-gain and loss terms modified NLCMEs with saturable gain and loss terms (NLCME+GL):

$$j\,\partial_z u + j V_g^{-1}\,\partial_t u + \kappa v + \Gamma(|u|^2 + 2\,|v|^2)u - j\,\tfrac{1}{2}\,[g\,(z,t) - l]\,u = 0, \tag{1a}$$

$$-j\,\partial_z v + j V_g^{-1}\,\partial_t v + \kappa u + \Gamma(|v|^2 + 2\,|u|^2)v - j\,\tfrac{1}{2}\,[g\,(z,t) - l]\,v = 0, \tag{1b}$$

where $u(z,t)$ and $v(z,t)$ are the slowly varying amplitudes of the coupled waves with positive and negative phase velocities,

respectively, κ is the coupling coefficient, σ is proportional to the average refractive index change along the grating [12], $g(z,t)$ is the amplifier gain coefficient, l is the loss coefficient, Γ is the nonlinear Kerr coefficient, $V_g = c/n_{\text{eff}}$ is the group velocity in the absence of the grating, c is the velocity of light in vacuum, and n_{eff} is the effective refractive index. To model gain dynamics in EDFAs we used several assumptions as described in detail in Ref. [10]: (a) The amplifier is a three-level energy system; (b) the effect of the pumping on the gain during the pulse propagation is negligible; (c) the small-signal gain along the grating length is constant; and (d) amplified spontaneous emission can be neglected. Assumption (b) is valid since the duration of the pulses that we consider is on the order of 1 ns while the effective response time of the amplifier is on the order of 10–100 μs [13]. Assumptions (c) and (d) are valid since we consider a short enough amplifier that is pumped with high enough power such that all erbium atoms are excited before the pulse arrives. By using these assumptions, the gain coefficient is given by [10]

$$g(z,t) = g \exp\left[\frac{-\int_{t_s}^{t} P_s(z,s)\,ds}{E_{\text{sat}}}\right], \tag{2}$$

where t_s is an arbitrary time before the pulse arrives at the amplifier and that can be mathematically set to $t_s \to -\infty$, $E_{\text{sat}} = P_{s,\text{sat}}\tau$ is the saturation energy, $P_{s,\text{sat}}$ is the signal saturation power of the amplifier, τ is the spontaneous decay time, and $P_s(z,t) = |u(z,t)|^2 + |v(z,t)|^2$ is the instantaneous pulse power.

The total energy that passes through the amplifier at location z equals $E_s(z) = \int_{-\infty}^{+\infty} P_s(z,\tau)d\tau$. For a single pulse this energy equals the total pulse energy at location z. The change in the total energy along the BG-EDFA can be calculated by using Eqs. (1a), (1b), and (2):

$$\frac{d}{dz}\left[\int_{-\infty}^{+\infty} |u(z,\tau)|^2 - |v(z,\tau)|^2\,d\tau\right] = gE_{\text{sat}}\left\{1 - \exp\left[-\frac{E_s(z)}{E_{\text{sat}}}\right]\right\} - lE_s(z). \tag{3}$$

According to Eq. (3), a steady-state solution $E_s(z) = E_{s,0}$ can be obtained by setting the left-hand side of Eq. (3) to zero:

$$gE_{\text{sat}}\left[1 - \exp\left(-\frac{E_{s,0}}{E_{\text{sat}}}\right)\right] = lE_{s,0}. \tag{4}$$

A solution for $E_{s,0}$ exists for positive coefficients g and l such that $g > l$. In this case the total pulse energy does not change while propagating in the amplifier.

In order to study nonlinear pulse propagation in BG-EDFAs, we solve Eqs. (1) and (2) by using a numerical simulation that extends the split-step method described in Ref. [14] to include saturable-gain and loss terms. The parameters of the BG-EDFA are $n_{\text{eff}} = 1.45$, $\kappa = 9000\ \text{m}^{-1}$, $\Gamma = 5\ \text{m}^{-1}\ \text{kW}^{-1}$, $P_{s,\text{sat}} = 104\ \mu\text{W}$ [13], $\tau = 10$ ms [15], and hence $E_{\text{sat}} = 1.04\ \mu\text{J}$. The loss parameter equals $l = 0.5\ \text{m}^{-1}$, as estimated in experiments [6]. In all of our simulations, the initial pulse is a BS with energy $E_{s,0}$ that is an exact solution of Eq. (13a) for a uniform FBG with $g = l = 0$. Since quasisolitons are not equal to BSs, the pulse slightly changes its parameters at the beginning of the grating ($L \lesssim 1$ m). The time

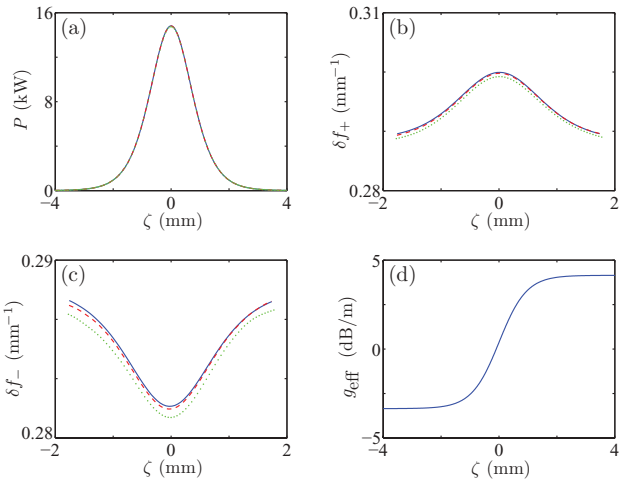

FIG. 1. (Color online) (a) Spatial pulse intensity $P(\zeta)$, wavenumber detuning from the Bragg wave number of the (b) forward propagating envelope u and (c) the backward propagating envelope v at the time when the center of the pulse is located at $z = 0$ (blue solid line), $z = 1$ m (red dashed line), and at $z = 5$ m (green dotted line) for an amplifier with a small signal gain g_0 of 3 dB/m. ζ is the location around the peak of the pulse. (d) shows the effective gain saturation $g_{\text{eff}} = (g - l)/v$ along the pulse at the time when the center of the pulse is located at $z = 5$ m. The input pulse is a Bragg soliton with parameters $\nu = 0.2$, $\rho = 0.114$, and with energy $E_0 = 0.68E_{\text{sat}}$.

$t = 0$ is defined as the time when the pulse center propagates 4 m in the BG-EDFA. The location of the pulse center at $t = 0$ is defined as $z = 0$. The pulse shape at the time when the center of the pulse is located at $z = 0$, 1, and 5 m is shown in Fig. 1 for an amplifier with a small signal gain g_0 of 3 dB/m and

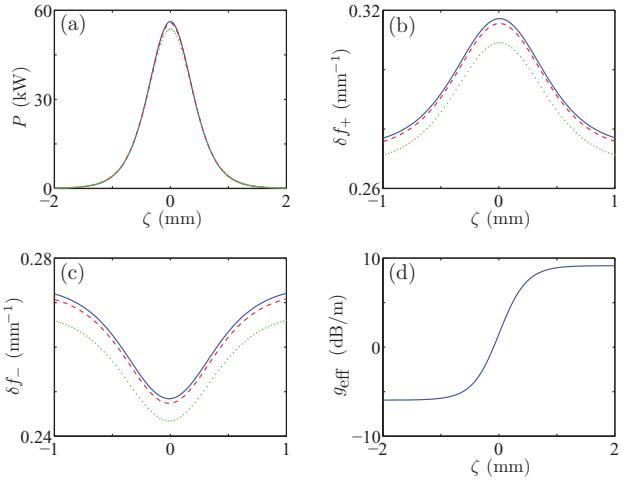

FIG. 2. (Color online) (a) Spatial pulse intensity $P(\zeta)$, wavenumber detuning from the Bragg wave number of the (b) forward propagating envelope u and (c) the backward propagating envelope v at the time when the center of the pulse is located at $z = 0$ (blue solid line), $z = 1$ m (red dashed line), and at $z = 5$ m (green dotted line), for an amplifier with a small signal gain g_0 of 5 dB/m. (d) shows the effective gain saturation along the pulse at the time when the center of the pulse is located at $z = 5$ m. The input pulse is a Bragg soliton with parameters $\nu = 0.2$, $\rho = 0.228$, and with an energy $E_0 = 1.37E_{\text{sat}}$.

in Fig. 2 for an amplifier with $g_0 = 5$ dB/m. The obtained pulse energy equals $0.68E_{\rm sat}$ for $g_0 = 3$ dB/m and $1.37E_{\rm sat}$ for $g_0 = 5$ dB/m. These results are in accordance with the steady-state solution of Eq. (3). The initial normalized group velocity of the pulse v equals 0.2 in both figures.

Figures 1 and 2 show (a) the spatial pulse intensity $P(\zeta)$ and the wave-number detuning from the Bragg wave number of (b) the forward propagating envelope u and (c) the backward propagating envelope v, as a function of the location, at the time when the center of the pulse is located at $z = 0$ (blue solid line), $z = 1$ m (red dashed line), and at $z = 5$ m (green dotted line). ζ is the relative location with respect to the peak of the pulse. The wave-number detuning from the Bragg wave number of the wave envelopes u and v is defined as $d\phi/dz$, where ϕ is the phase of the envelopes u and v, respectively. Figures 1(d) and 2(d) show the effective gain saturation along the pulse, $g_{\rm eff} = (g - l)/v$. Although significant gain saturation occurs along the pulse, no noticeable change in the pulse amplitude is observed when the center of the pulse propagates from $z = 0$ to $z = 1$ m.

Unlike BS that can theoretically propagate in FBGs without changing their shape, our numerical simulations indicate that the parameters of the quasisolitons that propagate in BG-EDFAs change slighlty during the propagation. The change becomes more significant as the saturation becomes stronger, as shown in Fig. 2. Figure 3 shows the relative change of the pulse amplitude and of the full width at half maximum (FWHM) of the spatial profile of the pulse. The parameters are the same as those used in Fig. 1. The peak power decreases during the propagation and the relative peak-power error after the center of the pulse propagates from $z = 0$ to $z = 5$ m is ~0.6% in case shown in Fig. 1 and 4.4% in case shown in Fig. 2. The FWHM of the pulse increases as the propagation length increases, as shown in Fig. 3. The overall energy of the pulse does not change, as obtain from the steady-state solution of Eq. (3).

Unlike BSs in uniform FBGs that propagate with a constant velocity, the velocity of the pulse that propagates in a BG-EDFA decreases during its propagation. We have numerically evaluated the normalized averaged energy velocity of the pulse as a function of its location along the BG-EDFA [10]:

$$v_{\rm e}(z) = \frac{\int_{-\infty}^{+\infty}[|u(z,\tau)|^2 - |v(z,\tau)|^2]d\tau}{\int_{-\infty}^{+\infty}[|u(z,\tau)|^2 + |v(z,\tau)|^2]d\tau}. \quad (5)$$

The result shown in Fig. 4 indicates that the pulse gradually reduces its velocity by ~0.05% per meter of propagation for the example shown in Fig. 1 and by ~0.5% per meter for the example shown in Fig. 2. We have verified that the total pulse energy does not change along the propagation. Hence, the slowing down of the pulse decreases its amplitude as shown in Figs. 1(a) and 2(b).

The resolution in both time and space domain was chosen to be $\Delta z = 0.005$ FWHM and $\Delta t = 0.005$ FWHM$/V_{\rm g}$, respectively, where FWHM is the spatial fFWHM of the pulse. We note that further reducing the resolution did not cause a smaller change in quasisoliton parameters.

Figure 5 shows the pulse profile and the wave-number detuning of the quasisoliton at $z = 0$ for the case shown in Fig. 2 that is compared to a BS solution in a uniform grating without gain or loss. The parameters of the BS were obtained by requiring that the BS energy and its central frequency will be the same as those of the quasisoliton that propagates in the BG-EDFA. Excellent agreement between the spatial pulse intensity profile and wave-number detuning was obtained between the BS and the pulse at a BG-EDFA. This result is not straightforward since the front end of the pulse that propagates in the BG-EDFA experiences a net gain while the rare end experiences effective loss due to the combination of gain saturation and loss as shown in Figs. 1(d) and 2(d).

III. MULTISCALE ANALYSES OF THE NLCME+GL AND NEW SOLITARY WAVE SOLUTION

In order to gain insight into quasisoliton propagation that was obtained numerically, we have developed a reduced analytical model. In the limit of low-intensity pulses we have reduced Eqs. II to a couple of nonlinear equations by using a multiscale analysis. One of the propagation equations is a modified nonlinear Schrödinger (NLS) equation that includes loss and saturable gain terms. When the gain saturation also becomes small, we obtain a new family of approximate solitary-wave solutions. The use of a multiscale analysis to obtain BS in uniform FBGs was developed in Ref. [7]. In this paper we apply a multiscale analysis to derive the propagation equations of pulses in BG-EDFAs. We show that solitary waves can propagate in such adevice when gain saturation is small.

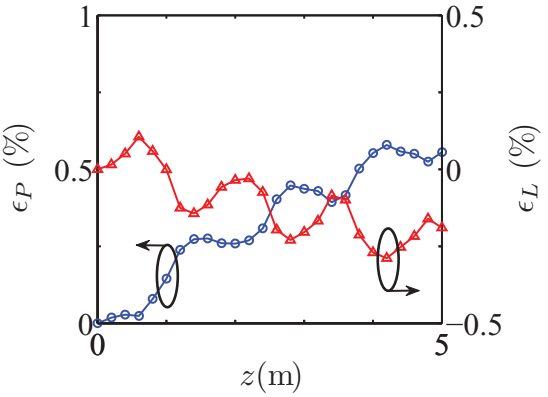

FIG. 3. (Color online) Relative change of the pulse amplitude ϵ_P and of the FWHM of the spatial profile of the pulse ϵ_L compared to the pulse at $t = 0$ as a function of the propagation distance z.

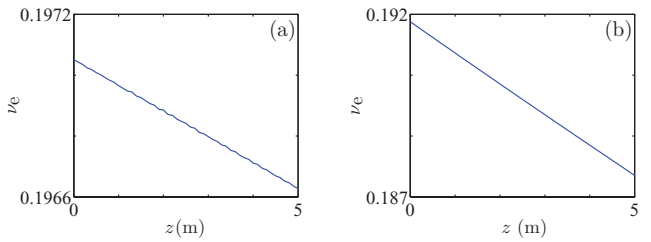

FIG. 4. (Color online) Evolution of the normalized energy velocity $v_{\rm e}$ of the pulse as defined in Eq. (5) as a function of the propagation distance for (a) the case shown in Fig. 1 and for (b) the case shown in Fig. 2.

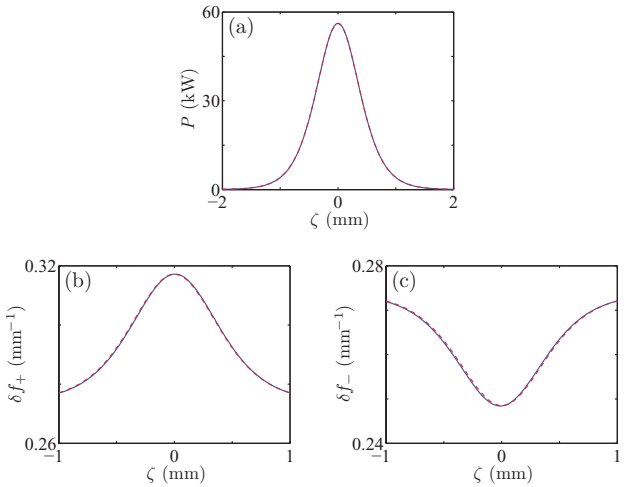

FIG. 5. (Color online) Comparison of (a) the pulse profile and the wave-number detuning from the Bragg wave number of (b) the forward propagating envelope u and (c) the backward propagating envelope v, between the quasisoliton shown in Fig. 2 at time $t = 0$ (blue solid line) and the fitted BS (red dashed line), with the parameters $\nu = 0.1922$, $\rho = 0.2173$. The fitted BS parameters were obtained by calculating the pulse group velocity ν from the results of the numerical simulation and comparing the expression for BS energy, $E_{\mathrm{BS}} = 4\rho(1-\nu^2)/(3-\nu^2)/(\Gamma V_{\mathrm{g}}\nu)$, to the steady-state energy, $E_{\mathrm{s},0}$.

The dispersion relation of a uniform grating without gain is obtained by substituting a continuous-wave solution into Eqs. (1) and requiring $g = l = \Gamma = 0$ [7]:

$$\mathbf{u}(\mathbf{z},\mathbf{t}) = \begin{pmatrix} u(z,t) \\ v(z,t) \end{pmatrix} = \mathbf{v}\exp\left[j\left(Qz - \Omega t\right)\right], \tag{6}$$

where Ω and Q are the frequency and wave-number offset with respect to the Bragg condition, respectively. We use bold notation to assign vectors. The dispersion relation equals

$$\Omega_{\pm} = \pm\frac{V_{\mathrm{g}}\kappa}{\sqrt{1-\nu^2}},\ Q = \frac{\kappa\nu}{\sqrt{1-\nu^2}}, \tag{7}$$

where $\nu = (1/V_{\mathrm{g}})d\Omega_+/dQ$ is the normalized group velocity. The corresponding eigenvectors are

$$\mathbf{v}_+ = \begin{pmatrix} \frac{\sqrt{1+\nu}}{\sqrt{2}} \\ -\frac{\sqrt{1-\nu}}{\sqrt{2}} \end{pmatrix},\quad \mathbf{v}_- = \begin{pmatrix} \frac{\sqrt{1-\nu}}{\sqrt{2}} \\ \frac{\sqrt{1+\nu}}{\sqrt{2}} \end{pmatrix}. \tag{8}$$

According to the method of multiscale analysis we introduce new coordinates that describe the wave evolution on different time and length scales: $t = t_0 + \mu t_1 + \mu^2 t_2 + \cdots$ and $z = z_0 + \mu z_1 + \mu^2 z_2 + \cdots$, where $0 < \mu \ll 1$ is a small parameter. To separate between the different time scales we need to make several assumptions. These assumptions are justified for low-intensity pulses similar to those used in experiments for demonstrating BSs [6]. We first assume that the carrier frequency of the propagating pulse is close to the upper edge of the band gap, i.e., $\Omega \approx \Omega_+ \approx V_{\mathrm{g}}\kappa$. We define the fastest time scale $T_0 \triangleq 2\pi\Omega^{-1}$. For moderate and strong uniform gratings, $\kappa \sim 1$–$10\ \mathrm{mm}^{-1}$ and T_0 is on the order of 1–10 ps. We define the shortest scale of the length $L_0 = 2\pi Q^{-1}$. T_0 and L_0 are related through phase velocity, as will be shown below. The variables t_0 and z_0 are the time and the location coordinates that vary on the time scale T_0 and the length scale L_0, respectively. We next assume that the spectral width of the propagating pulse is much smaller in comparison with the band-gap width. Therefore, we assume a solution,

$$\mathbf{u}(\mathbf{z},\mathbf{t}) = \mathbf{v}\left(z_1,z_2;t_1,t_2\right)\exp\left[j\left(Qz_0 - \Omega_+ t_0\right)\right], \tag{9}$$

where we choose

$$\mathbf{v}(z,t) = a(z_1,z_2;t_1,t_2)\mathbf{v}_+ + \mu b(z_1,z_2;t_1,t_2)\mathbf{v}_- + O(\mu^2). \tag{10}$$

Our third assumption is that the nonlinear length $L_{\mathrm{nl}} \triangleq [\Gamma\max(P_{\mathrm{s}})]^{-1}$, the gain length $L_{\mathrm{g}} \triangleq 1/g$, and the loss length $L_{\mathrm{l}} \triangleq 1/l$ are all on the order of $L_2 = \mu^{-2}L_0$. We therefore substitute in Eq. (1): $\Gamma \to \mu^2\Gamma$, $g \to \mu^2 g$, $l \to \mu^2 l$. The variables z_2 and t_2 are the spatial and the temporal coordinates that vary on the longest length scale L_2 and the longest time scale $T_2 = \mu^{-2}T_0$, respectively. The intermediate time and length scales are $T_1 = \mu^{-1}T_0$ and $L_1 = \mu^{-1}L_0$, respectively. We will show below that the length scale L_1 is connected to the time scale T_1 by the group velocity νV_{g}. We note that in the presence of the grating the nonlinear, gain, and loss distances are different in comparison with the above definitions due to the change in the propagation velocity of the pulse.

Our last assumption is that gain saturation does not depend on t_0 and z_0. The angular frequency of the propagating wave is $\Omega + \Omega_{\mathrm{B}}$, where Ω_{B} is the Bragg frequency. The bandwidth of the band gap is on the order of 1 nm while the bandwidth of the EDFA is on the order of 30 nm [13]. Therefore, the saturation term in Eq. (2), which is obtained by solving the rate equations [10], does not depend on the carrier frequency offset Ω and hence it does not depend on the fastest time scale t_0. Due to the slow response time of the EDFA and the propagation of the pulse, we also neglect the spatial hole burning effect and hence we neglect the dependence of the saturation on z_0.

We start separating the propagation equation into different time scales by expanding the integral in Eq. (2) according to the multiscale expansion. We use the method described in Ref. [16] to expand the saturation term into its different orders:

$$g(z_1,z_2;t_1,t_2) = g\exp\left[\frac{-\int_{-\infty}^{t_1} P_{\mathrm{s}}(z_1,z_2;s_1,t_2)\,ds_1}{E_{\mathrm{sat}}} + O(\mu)\right]. \tag{11}$$

We substitute Eqs. (9)–(11) into Eqs. (1) and equate the terms of the same power in μ. The equation for the the zero order μ^0 is the same as the propagation equation for a continuous-wave signal in a linear grating without loss or gain ($g = l = \Gamma = 0$). Therefore, Ω and Q satisfy the dispersion relation given in Eq. (7).

Collecting terms on the order μ^1 results in the following set of equations,

$$\frac{\partial a}{\partial\tau_1} = 0,\quad b = -j\frac{1-\nu^2}{2\kappa}\frac{\partial a}{\partial\zeta_1}, \tag{12}$$

where $\zeta_i = z_i - \nu V_{\mathrm{g}} t_i$, $\tau_i = t_i$. Hence, up to the first order of μ, both envelope functions $a(\zeta_1,\zeta_2;\tau_1,\tau 2)$ and $b(\zeta_1,\zeta_2;\tau_1,\tau 2)$ propagate with a group velocity νV_{g} that is equal to that

obtained in a uniform grating without nonlinear effects, gain, and loss.

Collecting terms of the order μ^2 results in the following set of equations for $a(\zeta_1,\zeta_2;\tau_1,\tau 2)$,

$$j\frac{\partial a}{\partial \tau_2}+\frac{1}{2}\Omega''_+\frac{\partial^2 a}{\partial \zeta_1^2}+\Gamma_{\rm eff}|a|^2 a - jV_{\rm g}\left[g\exp\left(-\int_{\zeta_1}^{\infty}|a(s_1,\zeta_2;\tau_1,\tau_2)|^2\,ds_1/E_{\rm sat}\right)-l\right]\times a=0, \tag{13a}$$

$$j\frac{\partial a}{\partial \zeta_2}-\frac{\nu\sqrt{1-\nu^2}}{\kappa}\frac{\partial^2 a}{\partial \zeta_1^2}-\frac{1}{2}\Gamma\nu|a|^2 a=0, \tag{13b}$$

where $\Omega''_+=d^2\Omega/dQ^2$ and $\Gamma_{\rm eff}=V_{\rm g}\Gamma(3-\nu^2)/2$. Equation (13a) is a modified NLS that includes loss and saturated-gain terms. Equations (13a) and (13b) extend the equations obtained in Ref. [8], where it was assumed that $g=l=0$.

We note that Eq. (13a) is similar to the equation that describes passive mode locking in lasers with a slow saturable absorber and slow-gain saturation [17,18]. The model in Refs. [17] and [18] also contains the effect of gain dispersion or an intracavity filter. Its solution was obtained assuming that the gain dispersion does not equal zero. In our model we neglect the gain dispersion term since the bandwidth of the quasisolitons is negligible in comparison to the bandwidth of EDFA (≈20 nm).

We first solve Eq. (13a). In order to obtain an analytical solitary-wave solution we add an assumption that the saturation is small and hence the pulse energy, $E=\int_{-\infty}^{t}P_{\rm s}(z,s)\,ds\ll E_{\rm sat}$. In this case, Eq. (13a) becomes

$$j\frac{\partial a}{\partial \tau_2}+\frac{1}{2}\Omega''_+\frac{\partial^2 a}{\partial \zeta_1^2}+\Gamma_{\rm eff}|a|^2 a + j\left(-g_0+g_1\int_{\zeta_1}^{\infty}|a(s_1,\zeta_2;\tau_1,\tau_2)|^2\,ds_1\right)a=0, \tag{14}$$

where $g_0=(g-l)V_{\rm g}$ and $g_1=g/(E_{\rm sat}\nu)$. Motivated by the results of our numerical simulations such as those presented in Fig. 5, we choose the ansatz,

$$\tilde{a}=A\,\mathrm{sech}[B(\zeta_1-\delta\nu V_{\rm g}\tau_2)]\exp[(C\zeta_1-D\tau_2)], \tag{15}$$

where A,B,C,D, and $\delta\nu$ are real coefficients. Substituting Eq. (15) into Eq. (14) gives

$$A=\frac{g_0}{g_1}\sqrt{\frac{\Gamma_{\rm eff}}{\Omega''_+}}, \tag{16a}$$

$$B=\frac{g_0}{g_1}\frac{\Gamma_{\rm eff}}{\Omega''_+}, \tag{16b}$$

$$C=\frac{\delta\nu V_{\rm g}}{\Omega''_+}-\frac{g_1}{\Gamma_{\rm eff}}, \tag{16c}$$

$$D=\frac{1}{2}\left(\frac{V_{\rm g}^2\delta\nu^2-\frac{g_0^2\Gamma_{\rm eff}^2}{g_1^2}}{\Omega''_+}+\frac{\Omega''_+ g_1^2}{\Gamma_{\rm eff}^2}-\frac{2V_{\rm g}\delta\nu g_1}{\Gamma_{\rm eff}}\right), \tag{16d}$$

where $\delta\nu$ is a free parameter that will be defined by using Eq. (13b). Hence we have obtained solitary-wave hyperbolic-secant solutions to Eq. (14). Once ν is chosen, the pulse intensity profile is uniquely determined by the steady-state energy condition. Assuming a small saturation as used in obtaining Eq. (14),

$$E_{\rm s,0}\simeq 2E_{\rm sat}\frac{g-l}{g}=2A^2/B. \tag{17}$$

We note that Eq. (13a) can also be used to model nonlinear wave propagation in a slow saturable fiber amplifiers without a grating. In this case Ω''_+ represents the fiber dispersion and $\Gamma_{\rm eff}$ represents the fiber nonlinear coefficient. The solutions given in Eqs. (15) and (16) show that solitary-wave solutions exist for Eq. (13a) when the saturation effect is small. However, the calculation of the solitary-wave pulse parameters for an EDFA shows that such pulses cannot be obtained without adding a grating. For example, assuming a dispersion coefficient of 15 ps/km nm, a loss of 0.2 dB/km, a gain coefficient of 3 dB/m, and the saturation energy of 0.1 μJ, the obtained solitary-wave pulse width is on the order of 10^{-22} s. This unphysical result is obtained due to the small dispersion coefficient of the fiber without the grating.

To present the solution in a similar form to that used for BSs in Ref. [3], we rewrite the solitary-wave solution by using two BS parameters, ν and $\rho_{\rm eff}$. We require $B=\sin\rho_{\rm eff}\kappa/\sqrt{1-\nu^2}$, and by using Eq. (16) we obtain

$$\sin\rho_{\rm eff}=\frac{E_{\rm sat}V_{\rm g}\Gamma\nu(3-\nu^2)(g-l)}{2(1-\nu^2)g}. \tag{18}$$

Then, the solitary-wave solution becomes

$$\tilde{a}=\left(\frac{\kappa}{\Gamma\sqrt{1-\nu^2}}\right)^{1/2}\alpha\sin\rho_{\rm eff}\,\mathrm{sech}\left[\frac{\kappa\sin\rho_{\rm eff}}{\sqrt{1-\nu^2}}(\zeta_1-\delta\nu V_{\rm g}\tau_2)\right]\times\exp(C\zeta_1-D\tau_2). \tag{19}$$

The solution $\tilde{a}$ solves Eq. (14). The full solution a must also solve Eq. (13b). We look for a solution of the form $a=\tilde{a}\exp(jF\zeta_2)$. Clearly this solution also satisfies Eq. (14). Direct substitution into Eq. (13b) gives the following results:

$$C=0, \tag{20a}$$

$$-F+\frac{2\kappa\nu(\sin\rho_{\rm eff})^2}{\sqrt{1-\nu^2}(3-\nu^2)}+O[\sin\rho_{\rm eff}]^4=0. \tag{20b}$$

Equation (20a) defines the value of the parameter $\delta\nu$:

$$\delta\nu=\frac{2(1-\nu^2)^{3/2}g}{E_{\rm sat}V_{\rm g}\Gamma\kappa\nu(3-\nu^2)}. \tag{21}$$

The second equation can be solved only up to the third order in $\sin\rho_{\rm eff}$, as was also the case in Ref. [8]. This approximation is also consistent with our earlier assumption of small nonlinearity, which allowed us to make the substitution $\Gamma\to\mu^2\Gamma$. The solution for the parameter F is given by

$$F=\frac{2\kappa(\sin\rho_{\rm eff})^2\nu}{\sqrt{1-\nu^2}(3-\nu^2)}. \tag{22}$$

We note that relatively small values of $\rho_{\rm eff}$ do not necessary result in low peak-power pulses. For example, the fitted BS in case of Fig. 5 has a peak power of 56 kW while the detuning parameter is only $\rho=0.2173$.

Using Eqs. (12) and (15) and substituting $\zeta_i = z - \nu V_g t, \tau_i = t, \mu \to 1$, we obtain

$$\mathbf{u}(z,t) \simeq \frac{A}{\sqrt{2}} \operatorname{sech}[B(z-(\nu+\delta\nu)V_g t)] \exp\{j[(F+Q)z-(D+FV_g\nu+\Omega_+)t]\} \times \begin{pmatrix} (1+\nu)^{1/2}\{1+\frac{1}{2}j(1-\nu)\sin\rho_{\text{eff}}\tanh[B(z-(\nu+\delta\nu)V_g t)]\} \\ -(1-\nu)^{1/2}\{1-\frac{1}{2}j(1+\nu)\sin\rho_{\text{eff}}\tanh[B(z-(\nu+\delta\nu)V_g t)]\} \end{pmatrix}, \tag{23}$$

where the parameters A, B, D, F, $\delta\nu$, and ρ_{eff} are defined in Eqs. (16), (18), and (22).

Solution (23) has the same spatial dependance as the solution found in Ref. [8]. It was shown in that work that the solution that is obtained by using the multiscale analysis for the case when $g = l = 0$ is identical to the BS solution, when terms on the order ρ^3 and higher are dropped. Hence, the solution found in this work has the same spatial dependence as the BS of velocity ν and energy $E_{s,0}$ in cases when the BS peak power is limited. However, the solitary wave obtained in this work propagates with a group velocity that is $\delta\nu V_g$ higher than the group velocity obtained in the absence of saturable gain and loss. The solution also has a different temporal phase dependence than in the BS solution. The change in the propagation velocity can be explained by the fact that when the pulses propagate in the saturable amplifier, the front tail of the pulse is amplified while the rear tail of the pulse is attenuated. Therefore, the center of the pulse is shifted toward its front tail and the group velocity of the pulse slightly increases.

The analytical solution given in Eq. (23) was compared to the results of the numerical simulations. Figure 6 compares the results in case of low saturation, when the steady-state pulse energy equals $0.2E_{\text{sat}}$. The only free parameter of the analytical solution, ν, was extracted by calculating from the results of the numerical simulation the spatial frequency at the center of the pulse and by using the dispersion relation (7). A good agreement between the numerical simulation and the analytical reduced model was obtained for both the intensity profile and wave-number detuning. The discrepancy between the analytical solution and the results of the numerical simulations becomes larger when gain saturation increases. However, even in the case of high saturation, such as in the case shown in Figs. 2 and 5, an excellent fit can be obtained between the numerically calculated pulse and a BS solution, as shown in Fig. 5.

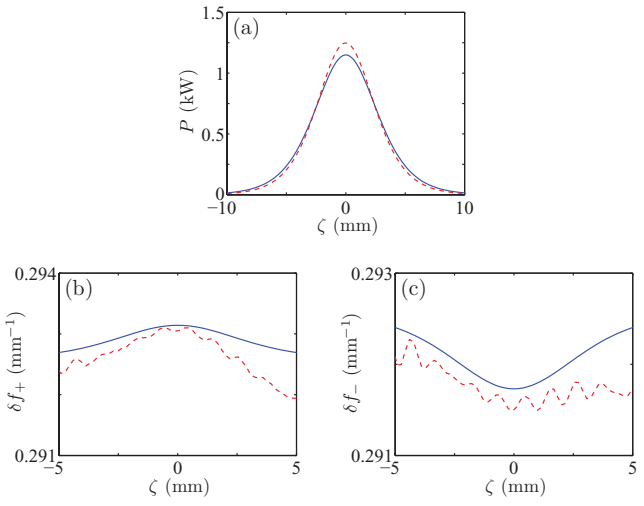

FIG. 6. (Color online) (a) Spatial intensity profile, wave-number detuning of (b) the forward propagating wave u, and (c) the backward propagating wave v after propagating 4 m in a BG-EDFA, calculated by using the numerical simulation (red dashed line), and by the analytical expression in Eq. (23) (blue solid line). The small signal gain equals $g = 0.27583\ \text{m}^{-1}$ and the steady-state pulse energy equals $0.2E_{\text{sat}}$. The free parameter of the analytical solution was obtained by calculating the spatial frequency near the peak of the pulse obtained using the numerical simulation.

We have also quantitatively compared the change of the group velocity of the reduced model to that obtained from the numerical simulation. For the parameters used in Figs. 1 and 2, the calculated normalized velocity increase $\delta\nu$ is on the order of 10^{-5}. This velocity change is too small to be verified by using the numerical simulation. By choosing another set of parameters, $g = 0.1522\ \text{m}^{-1}$, $l = 0.1446\ \text{m}^{-1}$, $E_{\text{sat}} = 10\ \mu\text{J}$, and $\kappa = 450\ \text{m}^{-1}$, and a pulse energy of $0.1E_{\text{sat}}$, we have obtained a normalized velocity increase $\delta\nu$ of 2.16×10^{-4}, as compared to $\delta\nu = 2.04 \times 10^{-4}$ obtained by using the numerical simulation.

IV. CONCLUSION

We have shown, by using a numerical simulation, that a quasisoliton can propagate over a very long distance in a FBG that is written in a slow saturable fiber amplifier, such as an erbium-doped fiber amplifier (BG-EDFA). The front end of the pulse experiences a net gain while the rear end of the pulse experiences a net loss due to the combination of gain saturation and loss. The spatial pulse profile is maintained symmetrical despite the significant change in the net gain along the pulse. However, unlike Bragg solitons, quasisolitons in BG-EDFAs slightly decrease their velocity and their central frequency during the propagation. By using a multiscale analysis, we developed a reduced model to study low-intensity pulse propagation in BG-EDFAs. The pulse propagation in the reduced model is described by two simple equations. One of the equations is a modified nonlinear Schrödinger equation that includes saturable gain and loss terms. When gain saturation becomes small, we were able to find analytically a new family of solitary-wave hyperbolic-secant approximate solutions. The obtained solutions have the same spatial dependence as BSs that propagate in uniform gratings without loss or gain, in

the limit of weak solitons. However, the pulses propagate slightly faster than in FBGs without gain or loss, due to gain saturation. The increase in the propagation velocity predicted by the analytical solutions as well as the spatial profile of the solutions were found to be in a good quantitative agreement with the results of the numerical simulation. The newly found quasisolitons may have a peak power on the order of tens of kilowatts. Such intense pulses are important for nonlinear applications such as frequency conversion.

ACKNOWLEDGMENTS

This work was supported by the Israel Science Foundation (ISF) of the Israel Academy of Sciences.

[1] W. Chen and D. L. Mills, Phys. Rev. Lett. **58**, 160 (1987).
[2] D. N. Christodoulides and R. I. Joseph, Phys. Rev. Lett. **62**, 1746 (1989).
[3] A. B. Aceves and S. Wabnitz, Phys. Lett. A **141**, 37 (1989).
[4] J. E. Sipe and H. G. Winful, Opt. Lett. **13**, 132 (1988).
[5] B. J. Eggleton, R. E. Slusher, C. M. de Sterke, P. A. Krug, and J. E. Sipe, Phys. Rev. Lett. **76**, 1627 (1996).
[6] J. T. Mok, C. M. de Sterke, I. C. M. Littler, and B. J. Eggleton, Nat. Phys. **2**, 775 (2006).
[7] C. M. de Sterke and J. E. Sipe, Phys. Rev. A **42**, 550 (1990).
[8] C. M. de Sterke and B. J. Eggleton, Phys. Rev. E **59**, 1267 (1999).
[9] I. C. M. Littler, T. Grujic, and B. J. Eggleton, Appl. Opt. **45**, 4679 (2006).
[10] Y. P. Shapira and M. Horowitz, Opt. Lett. **34**, 3113 (2009).
[11] H. Sakaguchi and B. A. Malomed, Phys. Rev. E **77**, 056606 (2008).
[12] T. Erdogan, J. Lightwave Technol. **15**, 1277 (1997).
[13] C. R. Giles and E. Desurvire, J. Lightwave Technol. **9**, 271 (1991).
[14] A. Rosenthal and M. Horowitz, Opt. Lett. **31**, 1334 (2006).
[15] K. Motoshima, L. M. Leba, D. N. Chen, M. M. Downs, T. Li, and E. Desurvire, IEEE Photon. Technol. Lett. **5**, 1423 (1993).
[16] Y. Inoue and K. Michihiro, J. Phys. Soc. Jpn. **50**, 681 (1981).
[17] H. A. Haus, IEEE J. Quantum Electron. **29**, 1228 (1993).
[18] F. X. Kärtner and U. Keller, Opt. Lett. **20**, 16 (1995).